Ring Puckering and CH Stretching Spectra. 3. High Vibrational States of Gaseous Monohydrogenated Cyclopentene-*4*-h_1

L. Lespade,* S. Rodin-Bercion, and D. Cavagnat

Laboratoire de Spectroscopie Moléculaire et Cristalline, URA 124, Université de Bordeaux I, 351 crs de la Libération, 33405 Talence Cedex, France

Received: August 5, 1996; In Final Form: December 3, 1996[⊗]

The excited CH stretching vibrational states of gaseous cyclopentene (4-HC_5D_7) have been measured from $\Delta v = 3$ to $\Delta v = 6$. Overtone spectra are modified by the large-amplitude ring-puckering motion and by a rapid energy flow to combination states. These two types of couplings with the CH stretching vibrations are explicitly modeled. The reconstruction of the spectra gives the predominant pathways of the intramolecular vibrational redistribution of the energy.

Introduction

Overtone spectroscopy has been recognized as a useful tool in the study of intramolecular dynamics of polyatomic molecules.[1−6] The interpretation of overtone spectra may give detailed insight into molecular high-energy states before photodissociation or laser-induced reaction. Indeed, it is well-known that energy in light atom stretch vibrations can rapidly flow from anharmonic high-frequency modes to other vibrational modes of the molecule. In particular, the very short time intramolecular vibrational redistribution (IVR) dynamics of CH overtones has been shown to be largely uncorrelated to the total state density[7,8] and to be governed by strong couplings with specific states: bending states in small molecules[9−24] or bending and wagging modes in hydrocarbons.[25,26]

In flexible molecules, the CH stretching vibrations are also modified by the large-amplitude motion. When the movement is slow enougth as in cyclohexene, there is no competition between the two phenomena, and the vibrational energy dynamics is essentially governed by the strong Fermi resonance couplings.[25] For more rapid motions, the two couplings have to be treated together.[27] For that purpose, the adiabatic approximation has proved to be a powerful tool to decouple the fast vibration from the slow large-amplitude motion in the first excited CH stretching state[28] as well as in higher overtones.[26] The coupling between the two motions can be described by an effective potential that contains a vibrational part corresponding to the variation of the vibrational energy during the internal motion. In the higher overtones, this vibrational part may become preponderant.

This paper is the third one of a series devoted to the study of the short time IVR in cyclopentene molecule.[26,29] In the first paper,[29] the theoretical basis has been established by ab initio calculations. In particular, the harmonic part of the variation of the vibrational energy as a function of the ring-puckering ccordinate (Figure 1) has been determined. For cyclopentene-*3*-h_1 (Cy3H), it is similar to the effective inversion potential resulting from the fitting of the first excited CH stretching spectrum. The difference between the "experimental" and calculated potentials can be attributed to the variation of the anharmonicity. For the CH bonds in the homoallylic position (on the carbon 4), there is a great discrepancy between the experimental and calculated data which could not be explained. The second paper of the series[26] is devoted to the excited vibrational states of cyclopentene-*3*-h_1. It shows that, because of the increasing part of the vibrational energy variation in the effective potential, there is a localization of the transitions in the two potential wells. Thus, the overtone spectra are mostly composed of bands corresponding to the two axial or equatorial positions of the CH bond. The spectra (from $\Delta v = 4$ to $\Delta v = 7$) are characterized by a large energy flow to combination states by Fermi resonances. This phenomenon has been modeled in curvilinear coordinates with the assumption that only the modes which give rise to important terms in the development of the kinetic energy have to be retained. A satisfactory reconstruction of the spectra has been obtained by solving an anharmonic Hamiltonian including the CH and CD stretching vibrations of the CHD methylene group attached to the carbon 3 and the two deformation modes of the angles adjacent to the CH bond where a frequency matching occurs. In particular, CC stretching ring modes and CD_2 bending modes have been disregarded. These modes are certainly also coupled with the CH stretching overtones but in a much weaker or indirect manner, and they only contribute to the broadening of the transitions.

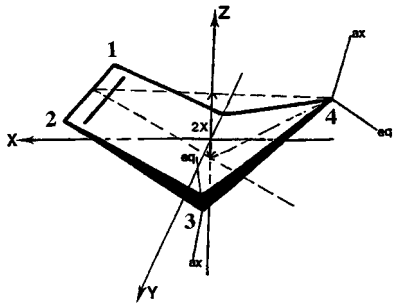

Figure 1. Definition of the ring-puckering coordinate x when the molecule is in its bent equilibrium conformation.

In this paper, the CH stretching overtone spectra of the cyclopentene-*4*-h_1 (Cy4H) are presented and analyzed in a slightly different but equivalent manner. After a brief description of the experimental conditions, the theoretical basis for the modeling of the spectra will be presented. The third section will be devoted to the discussion and analysis of the overtone spectra.

Experimental Section

Monohydrogenated cyclopentene-*4*-h_1 (4-HC_5D_7) was prepared by the organotin route according to the procedure described in ref 30. This method produces a mixed Cy4H and

[⊗] Abstract published in *Advance ACS Abstracts,* March 1, 1997.

S1089-5639(96)02364-X CCC: $14.00

Cy3H compound in approximately equal amounts, with an isotopic purity higher than 96% for the two compounds, as indicated by the analysis of the final compounds by ^{1}H, ^{2}H, and ^{13}C NMR, infrared, and mass spectroscopies. The product was degassed by the freeze−pump−thaw method and transferred under vacuum into the cells. The room-temperature vapor phase spectra were obtained by using two different techniques.

The near-infrared spectra ($\Delta v = 3-4$) were recorded by standard absorption spectroscopy on a Nicolet 740 FTIR spectrometer (resolution 1 cm^{-1}) between 3000 and 8600 cm^{-1} and a BioRad FTS-60A spectrometer (resolution 2 cm^{-1}) between 8600 and 11 500 cm^{-1}. The sample was contained in a Wilks cell ($l = 21$ m) equipped with CaF_2 windows. The sample pressure was between 50 and 200 Torr.

The visible spectra ($\Delta v = 5-6$) were recorded with the intracavity photoacoustic spectrometer which has been described elsewhere.[31] The pump laser is a 4 W Ar ion laser (Coherent Innova 70), chopped at 85 Hz. The photoacoustic cell is placed inside the cavity of a linear Coherent 599 dye laser. The spectral line width is 0.7 cm^{-1}, and the absolute wavelengths are measured with a PHO spectrometer to within ±2 cm^{-1}. We have used the following dyes: Pyridine 2 for the fourth overtone and DCM for the fifth one. For each spectrum (measured with a vapor pressure of 200 Torr) the Cy3H contribution was subtracted which was obtained from a pure product.[26] This subtraction is straightforward for the lower overtones but more difficult for the higher ones because of the broad features of the spectra. Nevertheless, it is made in order to cancel the axial absorptions of Cy3H which appear at lower frequencies, where no intense Cy4H absorptions are present.

Theoretical Approach

The theoretical approach in the analysis of the spectra has already been described in the first papers of the series.[26,29] Thus, we only briefly stress the important features. The coupling between the CH vibrations and the lower energy modes is treated in the adiabatic approximation, which means that the slow ring-puckering motion is temporally separated from the rapid vibrational motions.

As a consequence, the total wave function is the product of two wave functions describing the ring-puckering motion ($\psi(x)$) and the molecular vibrations ($\varphi(r,x)$) for every conformation of the molecule. The Schrödinger equation solving the total Hamiltonian H^T

$$H^T(x,q) = H^1(x) + H^2(q,x) \tag{1}$$

can thus be separated into two equations. The first one describes the fast vibrations for every geometry of the molecule, which means for every ring-puckering coordinate x (Figure 1). In the second, the ring-puckering potential is increased by the vibrational energy $e(x)$ which can be calculated by solving the vibrational equation.

Thus, for each overtone, the reconstruction of the spectra can be completed in two steps. First, the vibrational Hamiltonian including the anharmonic couplings with the HCD and HCC deformations is solved for each x position by diagonalizing the vibrational Hamiltonian matrix $H^2(q,x)$ for each manifold.

$$\sum_i H_{ji}^{\ 2}(v,x)\, c_{in}(v,x) = hc\omega_n(v,x)\, c_{jn}(v,x) \tag{2}$$

Then, the vibrational energies $hc\omega_n(v,x)$ are added to the ring-puckering potential $V_{\text{eff}}(0,x)$.

$$V^n_{\text{eff}}(v,x) = hc\omega_n(v,x) + V_{\text{eff}}(0,x) \tag{3}$$

The vibrational transitions between the two ring-puckering potentials $V_{\text{eff}}(0,x)$ and $V^n_{\text{eff}}(v,x)$ are calculated as explained in ref 29. Their intensities are obtained from the following relationship:

$$I^n_{|0,j\rangle\rightarrow|v,j'\rangle} = P\left(\int\int \varphi^*_v(r,x)\, \Psi^*_{vj'}(x)\, c_{1n}(v,x)\, \bar{\mu}(r,x)\, \varphi_0(r,x)\, \Psi_{0j}(x)\, \mathrm{d}r\, \mathrm{d}x\right)^2 \tag{4}$$

where P is the Boltzmann factor $\exp[-(E_{0j} - E_{00})/kT)]$ and $|0,j\rangle$ and $|v,j'\rangle$ are respectively the jth and j'th ring-puckering levels of the two effective potentials corresponding to the ground and excited states of CH bond stretchings. ψ_{vj} is the corresponding wave function of the ring-puckering Hamiltonian. $c_{1n}(v,x)$ is the eigenvector of the $\omega_n(v,x)$ contribution corresponding to the pure state with v quanta of CH stretching (with wave function φ_v). $\bar{\mu}$ is the dipole moment function. The integrals in x and in r of eq 4 can be separated if some assumptions are made: (i) The magnitude of the dipole moment transition is independent of the conformation. Contrary to what is observed in cyclohexane[32] or in nitromethane,[33] this assumption leads to a good fit to the observed $\Delta v = 1$ and 2 spectra of the two monohydrogenated cyclopentenes Cy3H and Cy4H.[29] (ii) The dipole moment is supposed to be collinear to the CH bond. As explained in ref 29, this fact can be verified in the simulation of the vapor phase contours of the two first excited vibrational spectra, and it gives a satisfactory result.

Finally, all the calculated spectra that correspond to the $\omega_n(v,x)$ where c_{1n} is not negligible are added to constitute the vibrational spectrum of the $(v - 1)$th overtone.

We have to notice that this procedure is slightly different from that used in ref 26 for Cy3H where the effective ring-puckering potentials are calculated by only introducing the vibrational energy contribution of ν_{CH} and by neglecting the anharmonic part of the vibrational Hamiltonian. The intramolecular energy flow by Fermi resonances is then calculated with the more intense transitions between the two effective potentials. We have verified that, for molecules such as monohydrogenated cyclopentenes, where the vibrational part of the effective potential leads to a strong localization of the transitions in the two potential wells corresponding to the axial and equatorial positions, the two procedures are equivalent.

Description of the Vibrational Hamiltonian. As stressed in ref 26, we have chosen to describe the vibrational anharmonic Hamiltonian in curvilinear coordinates because that is more adapted to large molecules such as cyclopentene. To model the Fermi resonance couplings, we have only retained modes that give rise to important anharmonic terms in the Taylor expansion of the kinetic energy matrix and added the corresponding potential part. In cyclopentene Cy4H, only two modes with adequate energy have to be taken into account: the two CH bending modes which correspond to deformations of the angles adjacent to the CH bond. Their wavenumbers are measured by infrared absorption at 1309 and 1270 cm^{-1}.[34] The former will be noted δ and the later one w.

The effective vibrational Hamiltonian is the sum of three terms:

$$H^2 = H^{20} + H^{21} + H^{22} \tag{5}$$

The zero-order Hamiltonian H^{20} describes the vibrations of the CH and CD bond stretchings as weakly coupled Morse oscillators and the deformation modes as weakly anharmonic oscillators.

$$\frac{H^{20}}{hc} = \sum_{i=1}^{2}\left\{\frac{1}{2}g^0_{rr}{p_{r_i}}^2 + D_i(x)(1 - e^{-a_i(x)r_i})^2\right\} + (g^0_{r_1r_2}p_{r_1}p_{r_2} + f_{12}(x)r_1r_2) + \frac{1}{2}(g^0_{\delta\delta}{p_\delta}^2 + f_{\delta\delta}(x)\delta^2 + f_{\delta\delta\delta}(x)\delta^3 + f_{\delta\delta\delta\delta}(x)\delta^4) + \frac{1}{2}(g^0_{ww}{p_w}^2 + f_{ww}(x)w^2 + f_{www}(x)w^3 + f_{wwww}(x)w^4) \quad (6)$$

Because of the partial deuteration, the deformation modes are described by quasi-pure symmetry coordinates.

$$\delta = \sum_{i=1}^{5}(L^{\delta}_{\theta_i})^{-1}\theta_i \qquad w = \sum_{i=2}^{5}(L^{w}_{\theta_i})^{-1}\theta_i \quad (7)$$

with θ_1 = HCD, $\theta_{2,3}$ = HCC, and $\theta_{4,5}$ = DCC. In these equations, $(L_{\theta i})^{-1}$ are the familiar $\mathbf{L}^{-1}$ matrix elements which give the dependence of normal modes in internal coordinates.

In the first- and second-order terms of the Hamiltonian, only the relevant expansions have been retained.[26] They correspond to the first and second derivatives of $g^0_{\theta_i\theta_i}$ in the displacement coordinates about the equilibrium configuration and the corresponding potential energy terms.

$$\frac{H^{21}_{\delta,w}}{hc} = \frac{1}{2}\sum_{i=1}^{5}\sum_{j=1}^{2}\left\{(L_i^{\delta,w})^{-2}\left(\frac{\partial g_{\theta_i\theta_i}}{\partial r_j}\right)_0 r_j{p_{\delta,w}}^2\right\} + \frac{1}{2}\sum_{i=1}^{5}\sum_{j=1}^{2}\{(L_i^{\delta,w})^2F_{r_j\theta_i^2}(x)(\delta^2,w^2)r_j\} \quad (8)$$

$$\frac{H^{22}_{\delta,w}}{hc} = \frac{1}{4}\sum_{i=1}^{5}\sum_{j=1}^{2}\left\{(L_i^{\delta,w})^{-2}\left(\frac{\partial^2 g_{\theta_i\theta_i}}{\partial r_j^2}\right)_0 r_j^2{p_{\delta,w}}^2\right\} + \frac{1}{4}\sum_{i=1}^{5}\sum_{j=1}^{2}\{(L_i^{\delta,w})^2F_{r_j^2\theta_i^2}(x)(\delta^2,w^2)r_j^2\} \quad (9)$$

The first-order term determines the Fermi resonance couplings $\lambda_{r\delta,w}(x)$, and the first and second terms determine the crossed anharmonicities $\chi_{r\delta,w}(x)$.[18,26] Because of the difference in the masses, they are different for the CH and the CD stretchings. In the reconstruction of the spectra, they are taken as fitting parameters because a small variation of the L_{θ_i} can lead to significant variations of the anharmonic potential parameters.

The total Hamiltonian matrix for every x value is calculated and diagonalized to obtain the $\omega_n(x)$. For that purpose, the variation of all the parameters during the motion must be known. These parameters are essentially the harmonic frequencies of the four modes (CH and CD stretching, bending and wagging vibrations), their anharmonicities, the cross-anharmonicities, and the Fermi resonance couplings. The harmonic frequencies of the bending and wagging modes and their variations have been taken from ab initio calculations. As stressed in ref 29, it was impossible to deduce the dependence of the stretching harmonic frequency upon the bond length variation determined by ab initio techniques. Thus, as most of the vibrational parameters, it has been obtained from the experimental spectra. Because of the localization of the principal transitions inside the two potential wells in the higher overtones, a crude reconstruction of the spectra have given the magnitude of all the parameters in the two axial and equatorial positions. The variation of the harmonic frequency of the CH stretching $\omega_0(x)$ has been calculated from the fitting of the first excited vibrational spectrum as explained in ref 29. Then, we have verified that the calculated spectra were only sensitive to the values of the other parameters in the two axial and equatorial positions. This is another proof of the strong localization of the transitions in the potential wells. As we could not estimate the values of these parameters outside the potential wells, the spectra have been modeled with linear variations.

Modeling of the Spectra. The vibrational Hamiltonian matrix is solved for every x value between −0.3 and 0.3 Å by steps of 0.02 Å. It is expanded in a basis set whose functions are products of Morse oscillator functions for CH or CD bond stretchings and harmonic oscillator wave functions for bending and wagging modes. The matrix elements are calculated for each basis function $|V\rangle = |\upsilon_{CH},\upsilon_{CD},\upsilon_\delta,\upsilon_w\rangle$ of all the possible combinations of the four modes corresponding to the $(\upsilon - 1)$th overtone. When the zero-point energy contribution is subtracted, the diagonal elements of the Hamiltonian expansion lead to the unperturbed energies:

$$\frac{1}{hc}(\langle\upsilon_{CH},\upsilon_{CD},\upsilon_\delta,\upsilon_w|H^{20}(x) + H^{21}(x) + H^{22}(x)|\upsilon_{CH},\upsilon_{CD},\upsilon_{CD},\upsilon_\delta,\upsilon_w\rangle) = (\omega_{0CH}(x) - \chi_{CH}(x))\upsilon_{CH} - \chi_{CH}(x){\upsilon_{CH}}^2 + (\omega_{0CD}(x) - \chi_{CD}(x))\upsilon_{CD} - \chi_{CD}(x){\upsilon_{CD}}^2 + (\omega_\delta(x) - \chi_\delta(x))\upsilon_\delta - \chi_\delta(x){\upsilon_\delta}^2 + (\omega_w(x) - \chi_w(x))\upsilon_w - \chi_w(x){\upsilon_w}^2 - \chi_{r_{CH}\delta}(x)\upsilon_{CH}\upsilon_\delta - \chi_{r_{CD}\delta}(x)\upsilon_{CD}\upsilon_\delta - \chi_{r_{CH}w}(x)\upsilon_{CH}\upsilon_w - \chi_{r_{CD}w}(x)\upsilon_{CD}\upsilon_w \quad (10)$$

There are two kinds of off-diagonal couplings: the Fermi resonance couplings which are deduced from the first-order Hamiltonian[25]

$$(1/hc)(\langle\upsilon_{CH},\upsilon_{CD},\upsilon_{\delta,w}|H^{21}(x)|\upsilon_{CH} - 1,\upsilon_{CD},\upsilon_{\delta,w} + 2\rangle) = \lambda_{r\delta,w}\sqrt{\upsilon_{CH}}\sqrt{(\upsilon_\delta + 1)(\upsilon_\delta + 2)} \quad (11)$$

and the interbond coupling between the CH and CD stretchings.

After the diagonalization of the Hamiltonian matrixes corresponding to each x value, the $\omega_n(x)$ and $c_n(x)$ are fitted by a least-squares method to a fourth-order polynomial form. The transitions between the two effective potentials ${V^n}_{eff}(x,\upsilon)$ and $V_{eff}(x,0)$ are calculated as described previously and added to form the calculated spectra of the $(\upsilon - 1)$th overtone. For that purpose, the dipole moment $\bar{\mu}(x)$ is decomposed in its components along the molecular principal axes determined by ab initio calculations.[29] The transitions corresponding to each (x,y,z) component are calculated with the appropriate theoretical vibration−rotation infrared contours[35,36] convoluted by a Lorentzian whose half-width is adapted to the experimental overtone spectrum.

Discussion

The overtone spectra of Cy4H from $\Delta\upsilon = 3$ to $\Delta\upsilon = 6$ are displayed in Figures 2−5. The best simulations of the spectra obtained with the parameters of Table 1 are also given. One can verify that the general trends of the experimental spectra are correctly reproduced.

As already noticed, the variation of the stretch harmonic frequency $\omega_0(x)$ was determined from the best fit of the first excited spectrum. We have tried to reproduce the spectra with a linear variation of the stretching anharmonicity and with that indicated in Table 1. The values of χ in each potential well were the same in both calculations. The resulting spectra were equivalent. This applies to all the other parameters. The fitting of the spectra only gives their values for the axial or equatorial positions (x = −0.12 or 0.12 Å) but in no way their exact variation during the motion. The uncertainty of the parameters

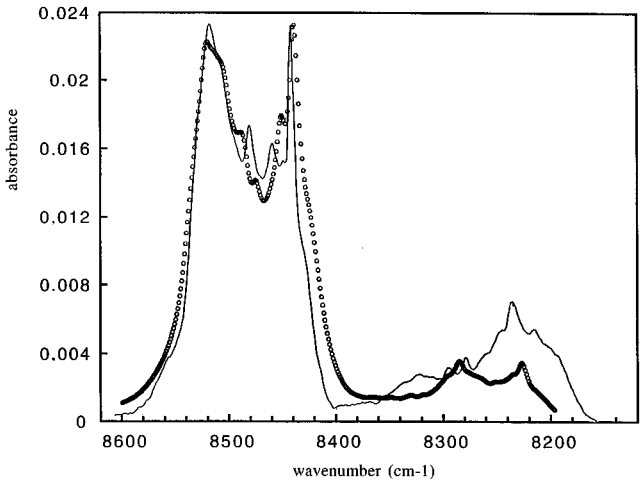

Figure 2. Observed and calculated spectra of the second CH stretching overtone ($\Delta v = 3$). The observed room-temperature spectrum (full line) was obtained by FTIR with a 21 m path length cell and a total pressure of 50 Torr. The circles represent the calculated profile with the theoretical band shapes obtained by convolution of the calculated ones at $\Delta v = 1$ with a Lorentzian of bandwidth 13 cm^{-1} (fwhm).

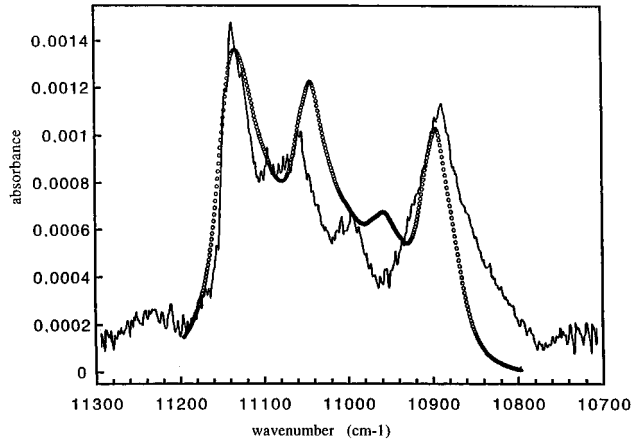

Figure 3. Observed and calculated spectra of the third CH stretching overtone ($\Delta v = 4$). The observed room-temperature spectrum (full line) was obtained by FTIR with a 21 m path length cell and a total pressure of 50 Torr. The circles represent the calculated profile with the theoretical band shapes obtained by convolution of the calculated ones at $\Delta v = 1$ with a Lorentzian of bandwidth 25 cm^{-1} (fwhm).

is difficult to evaluate because of their great number. The Birge−Sponer plot cannot give the exact diagonal anharmonicity because the Fermi resonance couplings with the bending and wagging combinations tend to raise the CH stretching wavenumbers in the first excited states ($\Delta v = 1-3$). Thus, we have tried to fit the spectra with different values of χ_{ra} and χ_{re}, and from the results of these fittings, we can assess that the uncertainty of these parameters is essentially about ± 0.5 cm^{-1}.

The values of the cross-anharmonicities involving the bending motion can be deduced from the combinations involving one quantum of bending vibration ($^3/_2$, $^5/_2$ and $^7/_2$ polyads in the notation of ref 6). They depend on the wavenumbers of CH stretching and of CHD bending vibrations and also on the Fermi resonance coupling. The former parameters are determined with a good accuracy. As a consequence, the uncertainty on the cross-anharmonicity is related to the determination of $\lambda_{r\delta}$. A 50% variation of the value of $\lambda_{r\delta}$ would modify $\chi_{r\delta}$ of ± 2 cm^{-1}.

The combination spectra with the wagging motion could not be observed. Thus, the parameters involving wagging motion are less easy to evaluate with a good accuracy. As they are not independent from each others, it is difficult to determine their uncertainty.

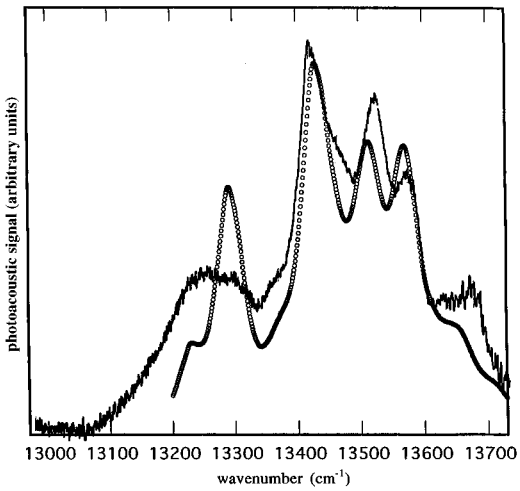

Figure 4. Observed and calculated spectra of the fourth CH stretching overtone ($\Delta v = 5$). The observed room-temperature spectrum (full line) was measured with the photoacoustic apparatus described in the text and a 11 cm path length cell. The total pressure of the sample was 200 Torr. The circles represent the calculated spectrum with the model described in the text. The line profiles were convoluted with a Lorentzian of bandwidth 25 cm^{-1} (fwhm).

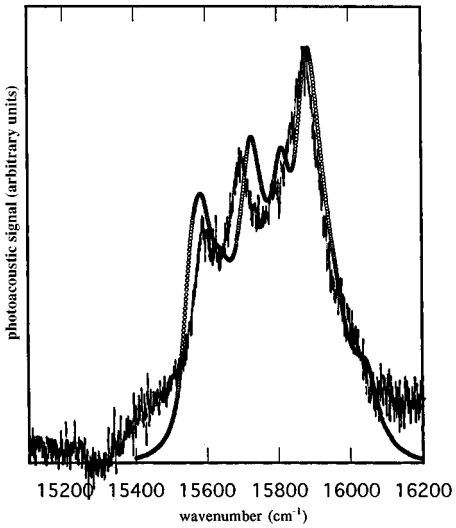

Figure 5. Observed and calculated spectra of the fifth CH stretching overtone ($\Delta v = 6$). The observed room-temperature spectrum (full line) was measured with the photoacoustic apparatus described in the text and a 11 cm path length cell. The total pressure of the sample was 200 Torr. The circles represent the calculated spectrum with the model described in the text. The line profiles were convoluted with a Lorentzian of bandwidth 40 cm^{-1} (fwhm).

In Table 1, only the effective parameters involving the CH vibrations are included, those involving the CD vibrations are not well determined by the fitting of the spectra. They have been deduced from the CH ones. In the same way, the interaction between the CH and the CD bonds is not efficient, contrary to what is observed in selectively deuterated dichloromethane[15] or nitromethane.[33]

The assignment of the observed peak absorptions is displayed in Tables 2 and 3. As for the Cy3H compound, there is a strong localization of the transitions in the two potential wells from the first overtones. Thus, the most intense transitions come from the axial $|0,0>$ or equatorial $|0,1>$ levels. (In that notation the first quantum number indicates the vibrational quantum number and the second the ring-puckering one.) We have to notice that the calculated wavenumbers indicated in Figures 2 and 3 correspond to the vibrational contribution in the effective potential $\omega_n(x)$ for the two axial and equatorial conformations.

TABLE 1: Effective Parameters Used in the Modeling of the Fermi Resonance Perturbed Spectra (Values for Axial and Equatorial Conformations Indicated by Subscripts a or e)

Local Parameters for CH Stretching Modes (cm^{-1})		
$\omega_0(x) = 3064 + 121.5x - 338x^2 - 2208x^3 + 21000x^4$	$\omega_{0a} = 3049$	$\omega_{0e} = 3077.5$
$\chi(x) = 63 - 7.5x - 69x^2 - 89x^3 + 2500x^4$	$\chi_a = 63.5$	$\chi_e = 61.5$
Effective Coupling between CH or CD Stretches (mdyn/Å)		
$f_{r1r2} = 0.05 \pm 0.01$		
Low-Frequency Mode Parameters (cm^{-1})		
$\omega_\delta(x) = 1316 - 150x^2 - 4150x^3 + 5000x^4$	$\omega_{\delta a} = 1332$	$\omega_{\delta e} = 1308$
$\chi_\delta(x) = 3.5 - 30x$	$\chi_{\delta a} = 7$	$\chi_{\delta e} = 0$
$\chi_{r\delta}(x) = 16.5 - 29x$	$\chi_{r\delta a} = 20$	$\chi_{r\delta e} = 13$
$\lambda_{r\delta}(x) = -79.5x + 16$	$\lambda_{r\delta a} = 21$	$\lambda_{r\delta e} = 12$
$\omega_w(x) = 1272 - 58x + 120x^2 - 1500x^3 + 4000x^4$	$\omega_{wa} = 1279$	$\omega_{we} = 1271$
$\chi_w(x) = 2$		
$\chi_{rw}(x) = 17.56 - 62.5x$	$\chi_{rwa} = 25$	$\chi_{rwe} = 10$
$\lambda_{rw}(x) = -139x + 22$	$\lambda_{rwa} = 30$	$\lambda_{rwe} = 17$

[a] The harmonic frequencies are directly deduced from the ab-initio calculations. The anharmonicities in the axial and equatorial positions are determined from the fitting of the spectra. All the other parameters are determined by fitting the experimental spectra excepted the variation of the wavenumber of the wagging motion in the first excited state which corresponds to that found by ab initio calculations.

TABLE 2: Observed and Calculated Fundamental Vibrations Involved in the Modeling of the Spectra[a]

ν(obs) (±0.5 cm^{-1})		fundamental vibrations		
IR	Raman	ν(calc) (cm^{-1})	eigenvector $c_1(x)$	assignt
1309	1305	1308		HCD def δ
1270		1257		eq HCC def w
		1276		ax HCC def w
2933	2933	2932	0.99 (−)	axial CH str
2958.5	2958.5	2959	0.99 (+)	eq CH str

[a] The eigenvectors are indicated by their values in the two potential wells (with the notation (−) for $x = -0.12$ Å and (+) for $x = 0.12$ Å).

They can be slightly different from the calculated transitions between the two effective potentials $V_{eff}(0,x)$ and $V^n_{eff}(\upsilon,x)$. Generally, the axial transition is higher by a few cm^{-1}. For example, the first excited axial transition is calculated at 2933 cm^{-1} with a vibrational contribution ω_1 (−0.12) of 2932 cm^{-1} (Table 2).

Effective Parameters. The calculations show that the coupling of the CH stretching with the ring-puckering motion contributes less and less to the redistribution of the energy with increasing excitation. The large flow observed for energies higher than 9000 cm^{-1} is essentially the consequence of strong Fermi resonances with combination states. One can notice from Table 1 that the Fermi resonance couplings are slightly different in the two positions of the CH bond. More generally, there is a discrepancy between the values of almost all the effective parameters in the two conformations contrary to what observed for Cy3H compound.[26] In the equatorial position, the anharmonic parameters involving both bending and wagging vibrations are of the same order of magnitude as those determined for Cy3H compound. On the contrary, these parameters are significantly larger in the axial conformation. The ab initio calculations had also evidenced a rather large variation of the HCC deformation wavenumber during the puckering motion which is reproduced by the effective parameters. It seems that the internal motion strongly modifies harmonic and anharmonic potentials of the vibrations attached to carbon 4, especially for the more constrained axial bond. This may be a consequence of the large-amplitude rocking of the homoallylic methylene group which has been evidenced by the ab initio calculations[29] to occur in phase with the puckering motion.

TABLE 3: Observed and Calculated CH Stretching Excited States[a]

ν(obs) (cm^{-1})	ν(calc) (cm^{-1})	eigenvector $c_n(x)$	assignt
	$\Delta\upsilon = 1.5$		
4 227	4 225	0.99 (−)	ax combin
4 256	4 255	0.99 (+)	eq combin
	$\Delta\upsilon = 2$		
5 744	5 741	0.96 (−)	ax 1st overtone
5 795	5 797	0.99 (+)	eq 1st overtone
	$\Delta\upsilon = 2.5$		
7 019	7 022	0.94 (−)	ax combin
7 075	7 083	0.98 (+)	eq combin
	$\Delta\upsilon = 3$		
8 240	8 226	0.35 (−)	ax combin
8 300	8 290	0.19 (+)	eq combin
8 441	8 431	0.89 (−)	ax 2d overtone
8 516	9 517	0.91 (+)	eq 2d overtone
	$\Delta\upsilon = 3.5$		
9 483	9 496	0.52 (−)	ax combin
	9 644	0.34 (+)	eq combin
9 711	9 710	0.82 (−)	ax combin
9 786	9 796	0.91 (+)	eq combin
	$\Delta\upsilon = 4$		
10 885	10 892	0.66 (−)	ax 3rd overtone
10 994	10 993	0.4 (+)	eq combin
11 055	11 038	0.63 (−)	ax 3rd overtone
11 094	11 065	0.45 (+)	eq combin
11 135	11 134	0.77 (+)	eq 3rd overtone
	$\Delta\upsilon = 5$		
13 236	13 221	0.29 (−)	ax combin
13 297	13 285	0.53 (−)	ax combin
13 414	13 419	0.63 (−)	ax 4th overtone
13 520	13 523	0.57 (+)	eq 4th overtone
13 571	13 574	0.58 (+)	eq 4th overtone
13 676	13 658	0.39 (+)	eq combin
	$\Delta\upsilon = 6$		
	15 555	0.39 (−)	ax combin
15 590	15 575	0.39 (−)	ax combin
	15 688	0.30 (−)	ax combin
15 700	15 725	0.48 (−)	ax 5th overtone
	15 803	0.32 (+)	eq combin
15 870	15 888	0.59 (+)	eq 5th overtone

[a] The eigenvectors are indicated by their values in the two potential wells (with the notation (−) for the axial position and (+) for the equatorial one).

Analysis of the Overtone Spectra. The modeling of the Fermi resonances with only two modes gives satisfactory results until 16 000 cm^{-1}. However, the transition intensities are less well reproduced than for Cy3H compound. One can notice that the Cy4H compound spectra exhibit more structured features than the Cy3H ones, especially in the higher overtones, which is not the signature of less energy redistribution. Indeed, the calculations evidence a slightly different redistribution of the vibrational energy. For each overtone, there are two or three $\omega_n(x)$ with $c_n(x)$ of comparable magnitude with that observed in Cy3H, and a large number of other components with weak eigenvectors that could not be observed. The Lorentzian half-widths (hwhm) by which we have convoluted the theoretical profiles are comparable to that used for Cy3H compound in the first overtones (13 and 25 cm^{-1} for $\Delta\upsilon = 3$ and 4) but less important in the higher overtones (25 and 40 cm^{-1} for $\Delta\upsilon = 5$ and 6). This could be linked to the absence of a third deformation mode weakly coupled to the CH stretching states which becomes efficient at $\Delta\upsilon = 6$ in the Cy3H compound.

Conclusion

We have measured the vapor-phase overtone spectra of cyclopentene Cy4H in the spectral regions corresponding to $\Delta v_{CH} = 3-6$. The interaction between the large-amplitude internal motion and the stretching vibrations can be modeled by a vibrational contribution to the ring-puckering effective potential. As for the other flexible molecules already studied,[26,33,37] because of its increasing asymmetry, this vibrational contribution is responsible for the localization of the transitions in each potential well. Thus, the energy flow which is observed for energies higher than 9000 cm^{-1}, is the consequence of Fermi resonances with isoenergetic combination states. The model we have elaborated, which includes all the possible combinations of the CH or CD stretchings with the two normal modes involving the deformations of the angles adjacent to the CH bond with adequate wavenumbers, leads to a satisfactory reproduction of the spectra, despite of the experimental mixture of Cy3H and Cy4H compounds, or theoretical difficulties since the ab initio calculations were not able to give the harmonic vibrational part of the effective potential with sufficient accuracy. This model shows that the deformation modes of the angles adjacent to the CH bond are the principal doorway states by which the vibrational energy is redistributed, in agreement with extensive previous investigations of anharmonic vibrational redistribution in the CH chromophore in symmetric and asymmetric top structural environments. The ring modes seem to have no strong anharmonic coupling with the CH stretching vibrations.

Acknowledgment. We are grateful to J. C. Cornut and J. J. Martin for assistance in experiments. We also acknowledge support of this research by the "Region Aquitaine" through the award of equipment grants.

References and Notes

(1) Dübal, H. R.; Quack, M. *Chem. Phys. Lett*. **1982**, *90*, 442.
(2) Dübal, H. R.; Crim, F. F *J. Chem. Phys.* **1985**, *83*, 3863.
(3) Ticich, T. M.; Likar, M. D.; Dübal, H. R.; Butler, L. J.; Crim, F. F. *J. Chem. Phys.* **1987**, *87*, 5820.
(4) Carpenter, J. E.; Weinhold, F. *J. Phys. Chem.* **1988**, *92*, 4295.
(5) Likar, M. D.; Baggott, J. E.; Crim, F. F. *J. Chem. Phys*. **1989**, *90*, 6266.
(6) Dübal, H. R.; Quack, M. *J. Chem. Phys*. **1984**, *81*, 3779.
(7) Lung, C.; Leforestier, C. *J. Chem. Phys.* **1992**, *97*, 2481.
(8) Luckhaus, D.; Quack, M. *Chem. Phys. Lett.* **1993**, *205*, 277.
(9) Quack, M. *Annu. Rev. Phys. Chem.* **1990**, *41*, 839.
(10) Quack, M.; Kutzelnigg, W. *Ber. Bunsen-Ges. Phys. Chem.* **1995**, *99*, 231.
(11) Baggott, J. E.; Clase, H. J.; Mills, I. M. *Spectrochim. Acta* **1986**, *42A*, 319.
(12) Baggott, J. E.; Chuang, M. C.; Zare, R. N.; Dübal, H. R.; Quack, M. *J. Chem. Phys*. **1985**, *82*, 1186.
(13) Segall, J.; Zare, R. N.; Dübal, H. R.; Lewerenz, M.; Quack, M. *J. Chem. Phys*. **1987**, *86*, 634.
(14) Green, W. H., Jr.; Lawrence, W. D.; Moore, C. B. *J. Chem. Phys.* **1987**, *86*, 6000.
(15) Baggott, J. E.; Law, D. W.; Mills, I. M. *Mol. Phys*. **1987**, *61*, 1309.
(16) Lewerenz, M.; Quack, M. *J. Chem. Phys.* **1988**, *88*, 5408.
(17) Halonen, L.; Carrington, T., Jr. *J. Chem. Phys*. **1988**, *88*, 4171.
(18) Halonen, L. *J. Chem. Phys*. **1988**, *88*, 7599.
(19) Halonen, L.; Carrington, T., Jr.; Quack, M. *J. Chem. Soc., Faraday Trans. 2* **1988**, *84*, 1371.
(20) Baggott, J. E.; Newnham, D. A.; Duncan, J. L.; McKean, D. C.; Brown, A. *Mol. Phys*. **1990**, *70*, 715.
(21) Ha, T. K.; Lewerenz, M.; Marquardt, R.; Quack, M. *J. Chem. Phys.* **1990**, *93*, 7097.
(22) Law, M. M.; Duncan, J. L. *Mol. Phys*. **1991**, *74*, 861.
(23) Davidsson, J.; Gutow, J. H.; Zare, R. N.; Marquardt, R.; Quack, M. *J. Phys. Chem*. **1991**, *95*, 1201.
(24) Hollenstein, H.; Luckhaus, D.; Quack, M. *J. Mol. Struct*. **1993**, *294*, 65.
(25) Lespade, L.; Rodin, S.; Cavagnat, D.; Abbate, S. *J. Phys. Chem*. **1993**, *97*, 6134.
(26) Rodin-Bercion, S.; Cavagnat, D.; Lespade, L.; Maraval, P. *J. Phys. Chem.* **1995**, *99*, 3005.
(27) Ticich, T. M.; Rizzo, T. R.; Dübal, H. R.; Crim, F. F. *J. Chem. Phys*. **1986**, *84*, 1508.
(28) Cavagnat, D.; Banisaed-Vahedie, S. *J. Chem. Phys*. **1991**, *95*, 8529. Cavagnat, D. *Thèse de Doctorat d'Etat, Bordeaux*, 1980.
(29) Lapouge, C.; Cavagnat, D.; Gorse, D.; Pesquer, M. *J. Phys. Chem.* **1995**, *99*, 2996.
(30) Cavagnat, D.; Banisaed-Vahedie, S.; Grignon-Dubois, M. *J. Phys. Chem*. **1991**, *95*, 5073.
(31) Lespade, L.; Rodin, S.; Cavagnat, D.; Abbate, S. *J. Phys., Colloq*. **1991**, *1*, C7−517.
(32) Gough, K. M.; Henry, B. R. *J. Phys. Chem.* **1984**, *88*, 1298.
(33) Cavagnat, D.; Lespade, L.; Lapouge, C. *J. Chem. Phys*. **1995**, *103*, 10502.
(34) Rodin-Bercion, S. Thesis, Université de Bordeaux, 1993. Lapouge, C. Thesis, Université de Bordeaux, 1996.
(35) Leicknam, J. C.; Guissani, Y.; Bratos, S. *Phys. Rev. A* **1980**, *21*, 1005.
(36) Leicknam, J. C. *Phys. Rev. A* **1980**, *22*, 2286.
(37) Cavagnat, D.; Lespade, L. *J. Chem Phys*., in press.